# Title

An AI-based and coding-free protocol for forests Leaf Area Index (LAI) calculation

# Author List

Tao Ma[1,2], Minxue Tang[3], Fangni Liu[1], Akwasi Duah-Gyamfi[4], Stephen Adu-Bredu[4], Mark Arcebal K. Naive[5,6], Imma Oliveras Menor[2,7], Sam Moore[2], Zhiyuan Zhang[8], Yadvinder Malhi[2,9]✉, Cecilia A. L. Dahlsj[2,9], Huanyuan Zhang-Zheng[2,9]✉

✉ Corresponding Authors

(yadvinder.malhi@ouce.ox.ac.uk)

(huanyuan.zhang@ouce.ox.ac.uk)

# Affiliations

1 College of Resources and Environmental Sciences, China Agricultural University, Beijing, China

2 Environmental Change Institute, School of Geography and the Environment, University of Oxford, Oxford, United Kingdom

3 Georgina Mace Centre for the Living Planet, Department of Life Sciences, Imperial College London, Silwood Park Campus, Buckhurst Road, Ascot, United Kingdom

4 Forestry Research Institute of Ghana, Council for Scientific and Industrial Research, Kumasi, Ghana

5 Center for Integrative Conservation and Yunnan Key Laboratory for Conservation of Tropical Rainforests & Asian Elephants, Xishuangbanna Tropical Botanical Garden, Chinese Academy of Sciences, Mengla, Yunnan 666303, China

6 University of Chinese Academy of Sciences, Beijing 100049, China

7 AMAP – botAnique et Modélisation de l'Architecture des Plantes et des Végétations, Université de Montpellier, CIRAD, CNRS, INRAE, IRD, Montpellier CEDEX 5, France

8 College of Resources and Environment, Fujian Agriculture and Forestry University, Fuzhou, Fujian 350002, China

9 Leverhulme Centre for Nature Recovery, University of Oxford, Oxford, United Kingdom

# Abstract

Measurements of Leaf Area Index (LAI) have become an important component in modern forest ecology and conservation. Detecting subtle annual, seasonal, and spatial variations in tropical forests is challenging, due to their complex structure and dynamic environmental conditions. Traditional processing of hemispherical photographs involves time-consuming pixel classification prone to subjective systematic errors, impeding comparison across months, years, and sites. While automated methods are available, they require coding expertise, which limits their adoption among non-specialists. We present a streamlined protocol that enables automatic, coding-free calculation of LAI by integrating two free software packages: ilastik, for AI-based pixel classification, and CAN-EYE, for LAI estimation.

To evaluate its performance, we compared the seasonal and spatial variations in LAI derived from our protocol with those from traditional pixel classification. Four sub-types of tropical forests were used to test the protocols, including moist evergreen forest, semi-deciduous forest, dry forests, and woody savanna. We found that traditional pixel classification (which requires manual threshold adjustments by operators) was influenced by subjective bias, with results varying depending on the time invested in pixel classification. In contrast, the fully automated workflow (our protocol: ilastik pixel classification + CAN-EYE calculation) eliminates subjective bias, enabling consistent cross-years and cross-operator comparisons. Validation using field photos and local forest phenology showed that the automated approach captured seasonal LAI variations more accurately than traditional processing, aligning with observed phenological patterns. However, analyses of spatial variation found no significant difference between protocols, as both captured site-to-site differences with comparable accuracy. Additionally, ilastik can classify pixels into non-binary categories (sky, leaves, and

twigs), providing additional detail that is useful for delineating savanna tree phenology. We present an automated, user friendly, and widely applicable protocol that enhances the accuracy, consistency, and reproducibility of LAI measurements, offering a robust tool for advancing tropical forest monitoring and research.

**Key words**: Leaf Area Index (LAI); digital hemispherical photography (DHP); machine-learning segmentation; ilastik; CAN-EYE; seasonal dynamics

# Introduction

Leaf Area Index (LAI) is widely used in climate change models, global carbon cycle assessments, and ecosystem restoration studies (Hazarika et al., 2005; Sumida et al., 2018; Veryard et al., 2023). Accurate measurements of LAI not only contributes to understanding of forests phenology, but also provides essential data supporting carbon cycle modeling (Li et al., 2019; Wang et al., 2024) laying the foundation for dynamically monitoring the response of complex ecosystems to climate change (Wu et al., 2024). Particularly in the context of global climate change, accurately capturing the spatiotemporal variations of LAI (Jiang et al., 2017) has become an essential research requirement in vegetation ecology and environmental science (Houborg et al., 2016; Ma et al., 2023). In tropical forests, LAI exhibits subtle but important spatial and temporal variation (de Wasseige et al., 2003; Malhado et al., 2009). Such variation is smaller than global scale variation but critically important for understanding the functioning of tropical forests. Tropical forests contain several subtypes including wet evergreen, semi-deciduous, dry forests, and more. Seasonality in wet evergreen tropical forests is not apparent to human eye, but such minor seasonal variations reveal the sensitivity of forest phenology to changes in climatic factors (Wu et al., 2017, 2016).

Accurately detecting these small fluctuations in LAI has always been a significant challenge (Li et al., 2024; Yan et al., 2019; Zou et al., 2023). Global products, such as the widely used MODIS product, are often critiqued after comparisons with field measurements (Zhang-Zheng et al., 2024b). Although drone-based remote sensing methods (Yan et al., 2024, 2021) provide large-scale LAI estimates, they typically rely on expensive LiDAR sensors or require powerful computing resources, creating significant financial barriers (Gara et al., 2021). Moreover, many remote sensing algorithms and models lack transparency in data and code, leading to poor reproducibility and exacerbating global disparities in research applications (Kedron and Frazier, 2022). Professional LAI measurement devices, for example Licor-LAI2200C, provide consistency but their prohibitive cost significantly limits widespread usage across resource-constrained institutes. Consequently, Digital hemispherical photography (DHP) methods through digital single-lens reflex (DSLR) cameras remain the primary ground-based approaches for quantifying forest LAI, especially in tropical regions. However, this approach faces a major challenge, among many others: each DHP image needs to be manually processed for sky-leaves pixel classification. This step is very time-

consuming and incurs strong subjective segmentation errors which affect consistency in cross-ecosystem studies (Fang et al., 2014).

The DSLR DHP method uses fisheye lenses to capture canopy images and, based on the segmentation of leaves and sky, calculates a ‘gap fraction’ to indirectly estimate LAI (Yang et al., 2023). Many algorithms have been proposed for this calculation, which introduce systematic errors to the absolute value of LAI, but not the pattern in seasonal or inter-annual variation. To delineate temporal (or spatial) pattern of LAI, it is crucial to ensure consistency in the segmentation step (i.e. the gap fraction step). However, subjective errors in the segmentation step impede cross-study comparisons (Jonckheere et al., 2004). Considerable variations exist among researchers in arbitrating the threshold for leaf-sky segmentation, leading to difficulties in standardising data across experiments and even across different years at the same site (due to change of personnel) (Pyare and Henning, 2012). Additionally, traditional DHP data analysis software (e.g., CAN-EYE) relies heavily on user input, requiring manual marking and parameter adjustments, which further exacerbates inconsistency (Gilardelli et al., 2018). Automatic image processing methods have been proposed. For instance, a MATLAB-based script was introduced to automate gap fraction analysis of digital canopy images (Fuentes et al., 2008). A modified image segmentation approach incorporating color space transformations and thresholding was developed to exclude non-leaf elements in fruit tree canopies (Carrasco-Benavides et al., 2016). These methods provide automation and thus theoretically avoid subjective bias, but the complexity of mathematical formulas and codes make them difficult to use for researchers without expertise in computer science (Chen et al., 2022). Consequently, these methods often lack reproducibility (Baker, 2016; Hoyt and Gyori, 2024) further exacerbating inconsistencies. There is therefore an urgent need to summarise the decades of LAI practice and establish a protocol that is free of subject errors, low-cost and coding free so that it can be widely applied for better standardisation of LAI measurements globally, and for decadal tracking of LAI.

In this paper, we are providing a protocol that leverages free, user-friendly software (ilastik and CAN-EYE) to minimise subjectivity in image segmentation. This protocol is specifically designed for a diverse user base, including forestry practitioners as well as undergraduate and graduate students seeking for cost-effective, reproducible LAI measurements with enhanced sensitivity to detect subtle LAI variation. The protocol has been applied in several forests ecological studies which manage to delineate subtle seasonal, spatial and annual variations in

forest LAI. To validate the protocol we will also conduct a comparison between the protocol and the traditional manual pixel classification method. Through comprehensive analysis of seasonal and spatial variation patterns across three representative tropical forest types (moist evergreen, semi-deciduous, and woody savanna), we show key operational limitations in manual methods while demonstrating the AI-driven automation significantly enhances measurement consistency.

# Methods

### *Case study site*

West African forests exhibit a well-defined ecological gradient, transitioning from coastal wet evergreen forests to savanna woodlands as they approach arid regions. To capture this diversity, our study sites encompass four distinct forest types: 1) wet evergreen, 2) semi-deciduous, 3) dry forests, and 4) woody savanna. The Ghanaian forests examined in this research are located at the eastern edge of the Upper Guinea forest, a biogeographic region separated from the Lower Guinea forest by the notable Dahomey Gap (Luiselli and Fa, 2019; Prance, 1984). West African forests show a pronounced ecological gradient from coastal wet evergreen forests to savannas with the latter exhibiting stronger rainfall seasonality than the former (Fig. 1). Our study focuses on three reserves along this gradient in Ghana (Table 1). Overall, there are 14 one-hectare plots, classified into four forests types and located in three natural reserves.

Study sites from part of the Global Ecosystem Monitoring (GEM) network (Malhi et al., 2021) and are registered in the ForestPlots.net database. Each monitoring plot (1-ha) was spaced at intervals ≥100 km between sites, providing a network for multi-scale LAI comparisons (both between-site vs. within-site variability).

### *Data Collection and processing*

In our case studies 25 hemispherical photo sampling points systematically distributed within each one-hectare plot. Note that the protocol mentions that the number of sampling points could be much less than 25. Details in Methods are describing the case studies. For the

protocol please check the link in supplementary. Photos were taken monthly from March 2012 to July 2019 for the study site BOB, while ANK and KOG initiated monitoring later. The dataset comprised, 19,044 hemispherical photos, demonstrating the methodological protocol's capacity for consistent processing of large image datasets. Following the protocol, this workflow generated 711 LAI values, as the CANEYE software outputs one value per plot-month combination. Spatial, seasonal, and interannual variations were analysed by averaging these values across relevant temporal scales. For interannual variation analysis, only years with more than four months of data were retained. To facilitate interpretation of seasonal LAI variation, representative field photographs and corresponding hemispherical images are shown (Fig. 2).

Across the study sites from ANK, BOB to KOG, a gradient of increasing rainfall seasonality was observed (Fig.1). The Seasonality Index (SI) was computed following this formula:

$$SI = (1/R) * \Sigma|Xj - R/12|$$

where Xj is monthly precipitation and R is total annual rainfall (Imteaz and Hossain, 2023).

We processed CHIRPS daily precipitation datasets (2000–2020) using Google Earth Engine(Funk et al., 2015), where we aggregated rainfall data to monthly totals, computed annual rainfall sums for each pixel, and derived the SI values for each year. The final output represents the 21-year mean SI, which characterizes long-term rainfall seasonality patterns across the study area.

Table 1. Key characteristics of study sites

| Study region | ANKASA (Wet) | BOBIRI | KOGYAE * | KOGYAE * |
|---|---|---|---|---|
| Latitude (°) | 5.2680 | 6.6910 | 7.2616 | 7.3012 |
| Longitude (°) | -2.6955 | -1.3389 | -1.1501 | -1.1649 |
| Elevation (m asl) | 114 | 235 | 229 | 221 |
| Forest Type | Evergreen | Semi-deciduous | Dry forest (DF) | Woody |

| | forest (EF) | forest (SDF) | | savanna (WS) |
|---|---|---|---|---|
| Mean Annual Precipitation | 2050 mm | 1500 mm | 1200 mm | 1200 mm |
| Plot Details | 3 × 1-ha plots (ANK-01–03) | 6 × 1-ha plots (BOB-01–06) | 2 × 1-ha plots (KOG-02–03) | 2 × 1-ha plots (KOG-05–06) |

*KOG-04 is a forest-savanna transition plot, it is included in the results but it does not belong to any of the four forest types.

# The protocol

The protocol provides a comprehensive, step-by-step guide for three key processes: 1) image segmentation (using ilastik), 2) LAI calculation (using CANEYE) and 3) LAI uncertainty quantification. To enhance usability, the protocol includes extensive annotated screenshots and instructional videos (Supplementary video). All software parameters for both ilastik and CANEYE are documented in detail within (Supplementary protocol). The protocol's strength include jargon-free explanations and minimal use of mathematical equations or programming code. Furthermore, it is compatible with low-tier commercial laptops without GPU acceleration. Ilastik is an open-source image analysis software that applies machine learning techniques (Berg et al., 2019). We selected both Ilastik and CANEYE because they are freely available and do not require programming expertise. However, users have the flexibility to combine ilastik outputs with alternative LAI estimation software packages (e.g., 'hemispheR', 'WinSCANOPY', 'hemisfer'). For comparative purposes, we present results from both our protocol (Approach 1) and the traditional CANEYE approach (Approach 2).

**Approach 1 The protocol workflow.**

In the protocol, we used ilastik to process fisheye photos which classified canopy and sky pixels into black and white. Note that CAN-EYE also has a function to classify pixels which is used in Approach 2 not Approach 1.

For the case study, we developed two distinct ilastik classification models: 1) a model trained on sites ANK and BOB (forests), and 2) a separate model for the KOG site (dry forests and

woody savanna). The methodological distinction was necessary due to fundamental differences in phenology: one of the KOG plots exhibited complete winter defoliation during the dry season (February), requiring a three-class annotation system (leaf, sky, branches) compared with the standard binary classification applied at ANK and BOB.

For model training, we randomly selected twenty fisheye photographs from each of the ANK and BOB sites. Pixel annotation was performed using the Pixel Classification workflow in ilastik, with manual labelling of leaf and sky pixels. The software then learned from these annotations to generate a classification model, which was applied in batch mode to process all fisheye images across all plots and months at both ANK and BOB sites. An identical workflow was implemented for KOG, with the modification of using the expanded three-category annotation scheme. Further details of the image processing steps are provided in the protocol section.

The black-and-white images classified by ilastik were organized by plot and month before being processed through the Binary DHP interface in CAN-EYE. It should be noted that CANEYE calculates a single LAI value per plot-month combination as standard output due to its algorithm (25 images per calculation in this study). CANEYE could not provide LAI for individual image.

Hereafter, results from the above processing are referred to as ‘the protocol’.

Approach 2: Leaf Area Index Measurement Based on CANEYE Color Image Processing interface following the Traditional workflow

In approach 2, we avoid Ilastik and use the pixel classification function embedded in CANEYE. The colored raw fisheye images were organized into plot-month folders and processed manually through CAN-EYE. Each folder contained 25 images. LAI values were calculated using the Color DHP (RGB) interface in CAN-EYE. Unlike approach 1, this method involved manual processing of a subset of plot-month folders (detailed below) due to the impracticality of processing all 19,044 images. The time-consuming nature is one of the drawbacks of approach 2. In approach 1, 40 images served as training data for developing two models (20 images per model), which were then applied to all 19,044 images. By contrast, approach 2 required manual processing of each individual image.

To demonstrate the impact of subjective errors on CANEYE results, we designed a controlled experiment incorporating three distinct time allocations for the pixel classification process: 30 seconds, 2 minutes, and ‘unlimited time’ per plot-month package. Note that in Approach 1, we spent much longer time (even longer than ‘unlimited time’) on each image to make the outcome almost perfect, simply because there we only have 40 images to process.

For all plot-month combinations in the ANK, BOB, and KOG forests post-January 2018, we implemented Color DHP processing where the pixel classification step was strictly limited to 2 minutes per plot-month package. During processing, we mainly marks 2-3 representative photographs from each 25-photo set for manual classification of sky and canopy elements. This experiment mimic typical CANEYE users scenarios.

For the ANK-01 and BOB-01 study plots post-January 2018, we implemented the following Color DHP processing (designated as ‘unlimited time’). This protocol imposes no restrictions on either the quantity of selected photos or the number of manual classifications performed per image. The process concludes only when the operator achieves full satisfaction with the sky-canopy classification accuracy. This experimental design replicates scenarios involving meticulous, perfectionist users, ensuring the highest possible classification quality.

For the ANK-01 and BOB-01 study plots post-January 2018, we implemented the following Color DHP processing (designated as ’30 seconds’). During the process, we mainly mark 1 photo from the 25 photos for manual classification, and this photo is manually classified 3-4 times on average. The classification takes exactly 30 seconds. This experiment mimic hasty users scenarios.

In this study, the operators conducting the CANEYE image segmentation experiment are not responsible for calculating the Leaf Area Index (LAI). During segmentation, they perform only manual sky-canopy classification without access to LAI-related results. At this stage, operators view solely the sky percentage data and do not receive the final LAI value. The LAI computation occurs post-segmentation, automatically by the software, ensuring the classification phase remains independent of LAI derivation. Consequently, the segmentation operators remain free from subjective bias, as their work in uninfluenced by LAI outcomes.

Hereafter, results from the above processing are referred to as ‘30 seconds’, ‘2 minutes’ and ‘unlimited time’.

# Results

### *Seasonal variation of LAI*

The study was conducted at three forest sites in Ghana, West Africa, each situated in areas with different rainfall seasonality (Fig.1), which resulted in differences in phenology. To aid in the interpretation of seasonal LAI variations, representative field and hemispherical photographs are shown (Fig. 2).

For the moist evergreen forest ANK-01, LAI of ‘the protocol’ exhibits clear seasonal variation. From April to July 2018 and March to July 2019, the LAI shows a noticeable seasonal increase, reaching its peak in July 2018 and July 2019, respectively. Between August and December 2018, the LAI remains in a fluctuating phase. In contrast, during January to April 2018 and December 2018 to February 2019, the LAI values are relatively lower (Fig. 3). These seasonal variations are consistent with the multi-year average for the study sites (Supplementary Figure 1).

In traditional CAN-EYE color image processing (approach 2), it is important to note that the results vary depending on the time spent on the operation. The suspected reason is that operators often mark up the sky first and then spend most of their time marking leaves and branches while iteratively checking the segmented images. Thus, the ‘30 seconds’ experiment likely missed some leaves due to time constraints. Ilastik does not have an ‘operation time’ issue since the random forest algorithm is highly efficient. It achieves excellent pixel classification with very few manual marks. Moreover, the training dataset for Ilastik is very small (ca. 20 photos), allowing the operator review every image to ensure precise segmentation. Because each month is processed independently in traditional CAN-EYE, there is more month-to-month variation compared to ‘the protocol’, which is less desirable since the seasonal variation of forest LAI should be smooth from a physiological perspective.

’30 seconds’ performed poorly in terms of both seasonal variation and underestimated LAI values (Fig. 3). In contrast, ‘2 minutes’ exhibits seasonal trend highly similar to those of ‘the protocol’. Nonetheless, statistical analysis confirmed that the LAI values from the ‘2 minutes’ are significantly higher than those obtained with ‘the protocol’ (Supplementary Figure 11 and Figure 13).

In the CAN-EYE traditional processing, both ‘2 minutes’ and ‘unlimited time’ found exceptionally high LAI values in September 2018. However, based on visual inspection of the color photographs (Supplementary Figure 2), it is more likely that July 2018 should have had the highest LAI. Additionally, such considerable fluctuations in LAI from July (high value), to August (low value) and back to September (very high value) are biologically implausible. In summary, our detailed seasonal comparison at the ANK01 site demonstrates that ‘the protocol’ provides more realistic results for seasonal variation.

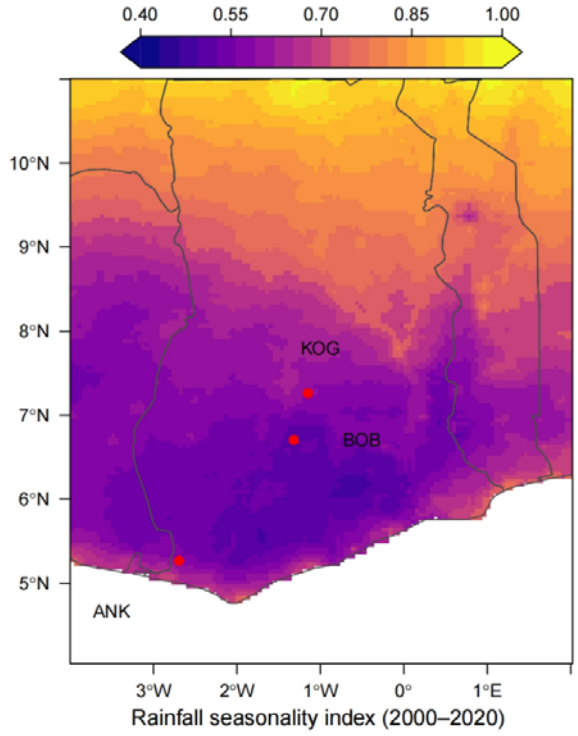


***Fig. 1 Map of the study site and rainfall seasonality index of Ghana, West Africa*** *. The background shows the seasonality index of rainfall. Typically, values smaller than 0.2 suggest no seasonality. Values around 0.45 suggest moderate seasonality with a short drier season. Values larger than 1.0 suggest most rainfall occur in less than 3 months* (Nair et al., 2014).

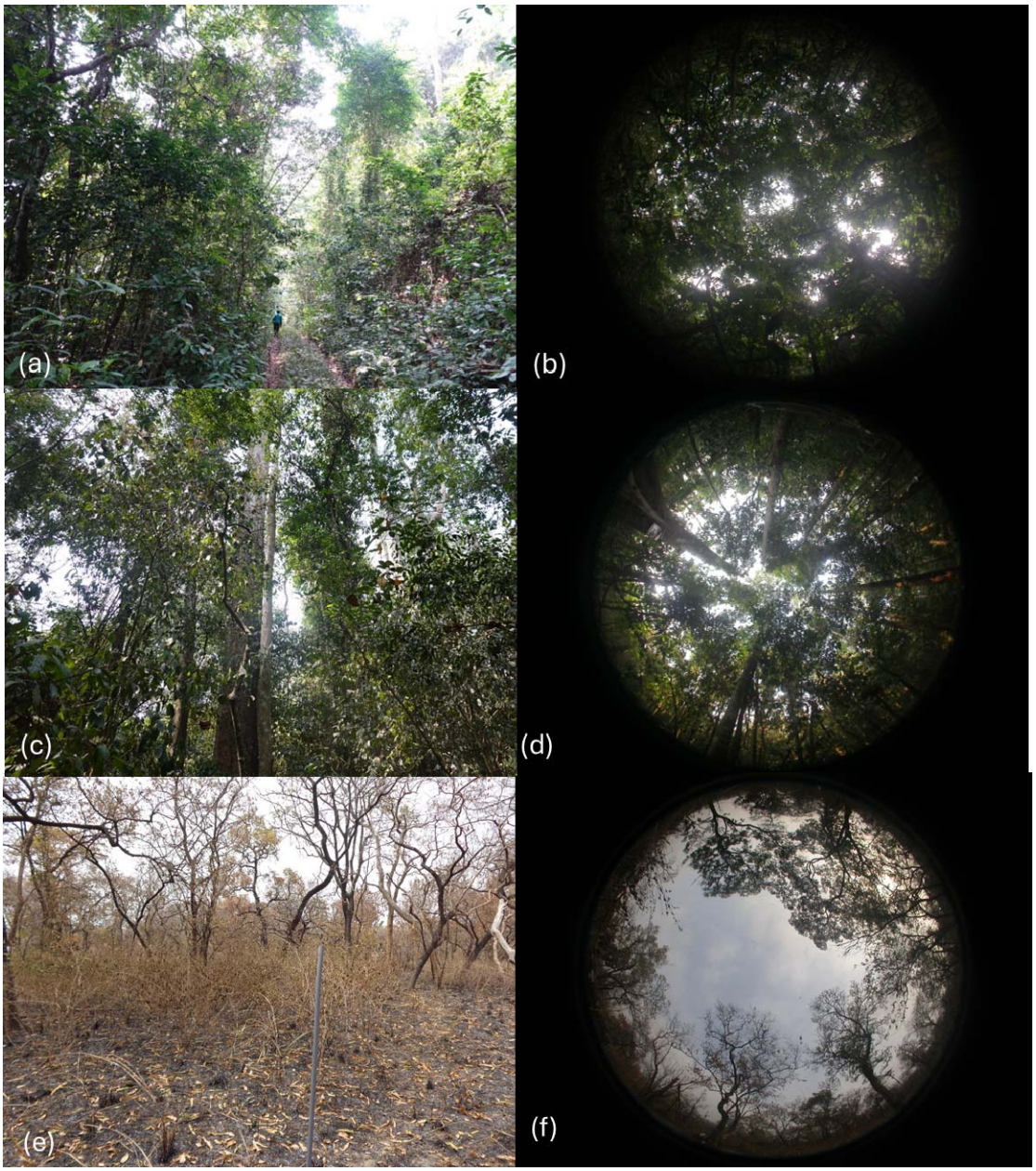


***Fig. 2 Photos of the study sites and examples of their hemispherical photos.*** *Here we show (a) the path leading to site ANK, at the entrance of ANK; (b) hemispherical photo of plot ANK01 in January 2019 (dry season); (c) study plot BOB-01 (d) hemispherical photo of BOB-02 in January 2019; (e) Study plot KOG-05 after fire (f) hemispherical photo of KOG-05 taken in 2019 January.*

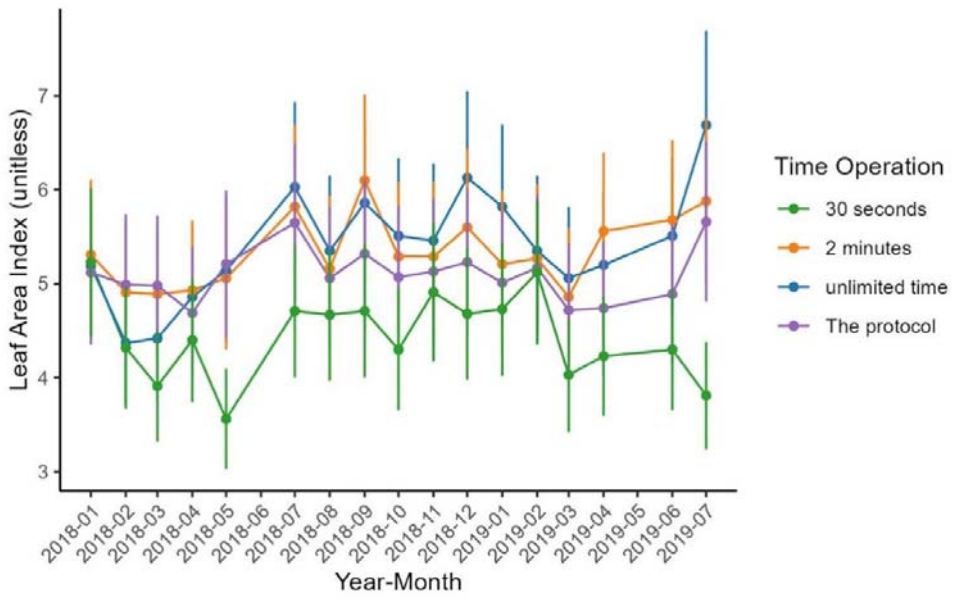


***Fig.3 Time series of Leaf area index for different experiment settings in the Ankasa National Forest (Moist Evergreen Forest) plot ANK-01****. The purple line represents the protocol, using ilastik to process images, which has no operation time as it only needs to be trained once. The remaining colours represent traditional manual image processing experiments (Approach 2). Error bars represent ± 15% of the mean.*

For the BOB-01 forest, both 'the protocol' and '2 minutes' methods showed very similar seasonal variations. It is particularly evident that from November 2018 to April 2019, the LAI values remained at very low levels. This result aligns well with the dry season months in southern Ghana (the dry season lasts from December to mid-March).

Statistical analysis shows that the LAI of '2 minutes' are consistently and significantly higher than those of 'the protocol' in most months (Supplementary Figure 11 and Figure 13), mirroring the pattern observed at ANK-01. In the careful processing (blue line), although the seasonal variation remains consistent, the LAI values are considerably higher than those from both 'the protocol' and '2 minutes'. The '30 seconds' operation (green line) produces LAI values considerably lower than those from 'the protocol' and '2 minutes'. (Fig. 4). Similar to the conclusion for ANK-01, the results are subject to operation time, and the traditional CAN-EYE method has more monthly fluctuation.

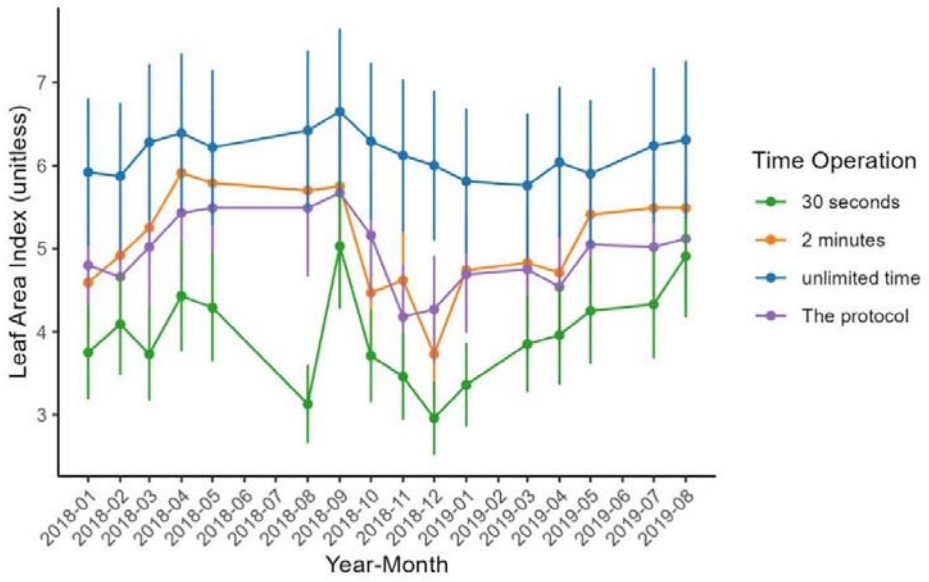


***Fig.4 Time series of Leaf area index (LAI) for different experiment settings in the Bobiri (semi-deciduous Forest) plot BOB-01.*** *The purple line represents the protocol, using ilastik to process images, which has no operation time as it only needs to be trained once. The remaining colours represent traditional manual image processing experiments (Approach 2). Error bars represent ± 15% of the mean.*

For the KOG forest, both 'the protocol' and '2 minutes' showed similar seasonal variation. LAI of '2 minutes' is significantly higher than that of 'the protocol' at KOG-02 and KOG-03. No significant difference was found for other KOG plots (Supplementary Figure 12). At KOG, some of the photo sampling points feature a large sky window. Hence, each month-plot package comprises pictures with and without large sky windows. CAN-EYE set a constant threshold for the whole package which often fails to process the two distinct types of photos (Supplementary figure 5). When the marking is drawn for closed canopy photos, a portion of the large sky window is often mistaken as leaves, leading to over-estimation of LAI. In contrast, ilastik avoids this dilemma entirely, significantly reducing processing time.

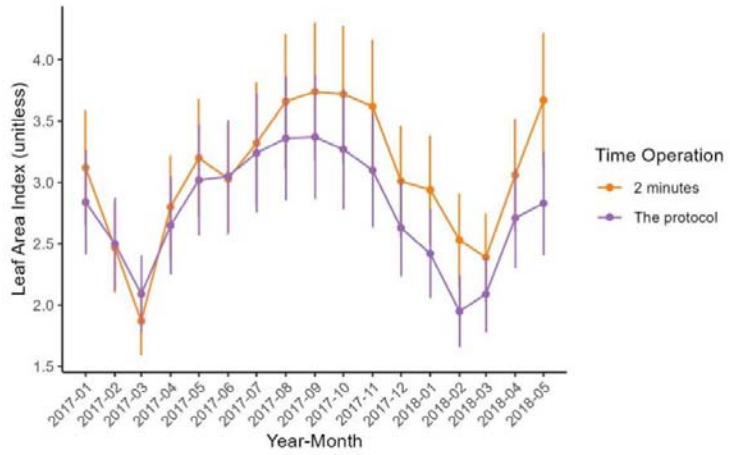


(a)

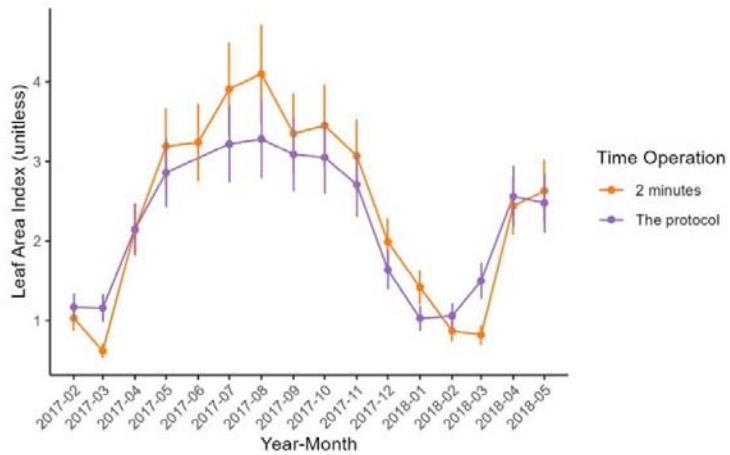


(b)

***Fig.5 Time series of Leaf area index (LAI) for different experiment settings in the Kogyae (dry forest).*** *The purple line represents the protocol which uses ilastik to process images. It has no operation time as it only needs to be trained once. The orange line represents the two-minute processing experiment (Approach 2).* ***(a)*** *KOG-02 forest(dry forests) ;* ***(b)*** *KOG-06 forest(woody savanna). Error bars represent ± 15% of the mean.*

### *Spatial and inter-annual variation of LAI*

When compared to the ANK and BOB forests, the KOG forest sites exhibits a lower LAI, consistent with its ecotone position between dry forests and savanna. For ‘the protocol’, the highest LAI value occurs at ANK-03, whereas for ‘2 minutes’, the highest LAI is found at the BOB-04 site (Fig. 6). The difference between BOB-04 and ANK-03 is difficult to discern through visual inspection of the color photographs (Supplementary Figure 6), and these two

plots have very similar stem biomass (Zhang-Zheng et al., 2024a). Additionally, statistical analysis confirmed that the LAI values obtained from 'two minutes' are consistently—and significantly—higher than those derived from 'the protocol', as discussed above (Supplementary Figure 12). Overall, both 'the protocol' and 'two minutes' demonstrate a reasonable pattern of LAI variations between plots (Fig. 6), which aligns with the biomass variation of these plots (Zhang-Zheng et al., 2024a). For inter-annual variation, a comparison between '2 minutes' and 'the protocol' was not possible due to insufficient manpower to to manually process 19,044 images. Nonetheless, using 'the protocol', we demonstrated that ANK and BOB experienced an increase in LAI over time, while KOG showed a decrease (Fig. 7). Forest plots within each site are separated by only several kilometers, so we would expect to see similar inter-annual variation in LAI.  As expected, the inter-annual pattern is consistent among plots within each study site. For BOB and KOG, we found that LAI declined in 2016, consistent with the 2015/2016 El Nino event.

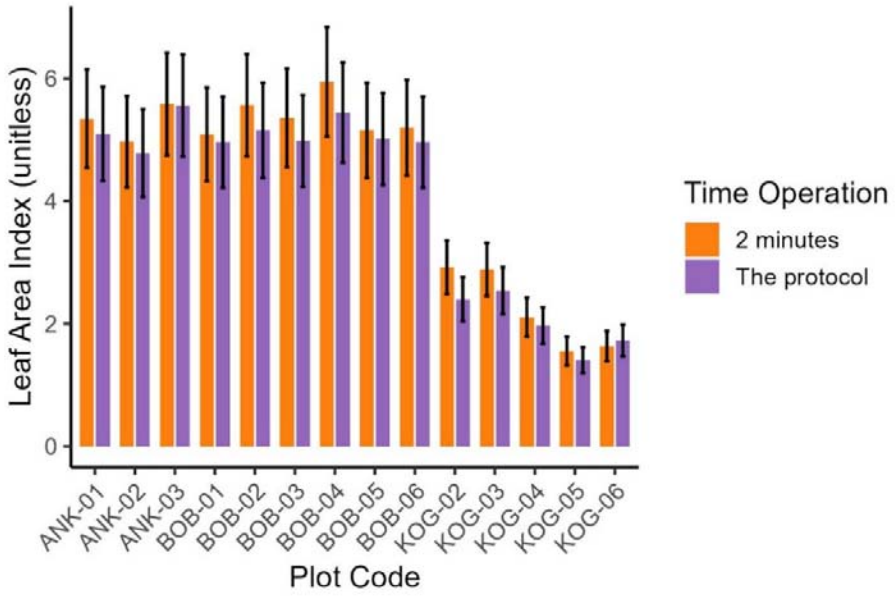


***Fig.6 Comparison of LAI between 2-minutes processing experiment and the protocol (fully automated using ilastik) across different forest plots.*** *The orange bars represent CAN-EYE 2-minute processing, while the purple bars represent ilastik fully automated processing. The Plot Code includes ANK (Moist Evergreen Forest), BOB (Semi-Deciduous Forest), KOG 02-03 (Dry Forest) and KOG 05-06 (Savanna). Error bars represent ± 15% of the mean.*

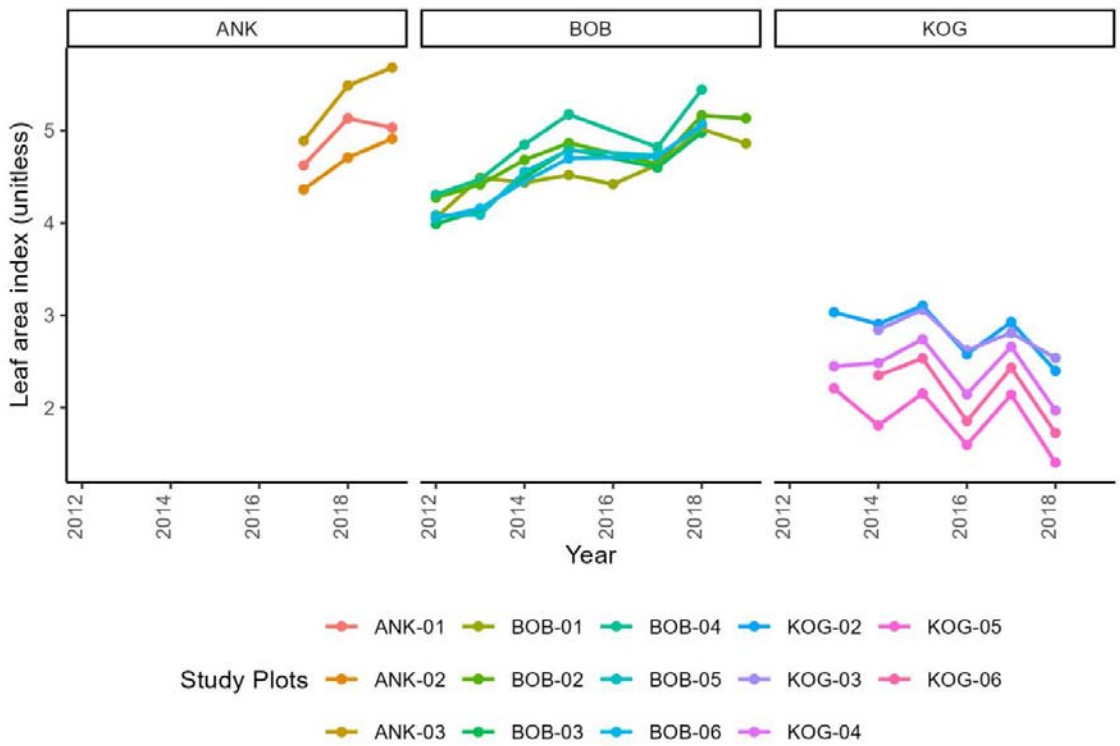


***Fig.7 Inter-Annual Variation Of Leaf Area Index Following The Protocol.*** *Different colours represent study plots.*

# Discussion and conclusion

### *The traditional manual pixel classification*

This study reveals that the traditional manual pixel classification process introduces a strong systematic bias in LAI estimates. Variations among different operators arise when processing the same image, depending on the time spent on annotation, their experience, and subjective judgment criteria.

First, a ‘grey zone’ exists at the edge of leaves (Supplementary Figure 7) where human eye could not identify whether the pixels belong to leaves or sky. When performing manual

classification, operators must arbitrate for these grey zones. However, sun-bleached leaf edges or light green areas are often misclassified as sky, which reduces the reliability of the data. Previous studies have demonstrated that human judgment in complex scenarios significantly impacts data results (Jonckheere et al., 2004). Consequently, more grey zones are identified as leaves when operators spend more time on leaf annotation, resulting in higher LAI values with increased working hours (Figure 4). For Ilastik, the AI also needs to find a middle ground for these grey zones. The AI's decision may not be precise, but it is consistent across years and sites.

Furthermore, field photographs often exhibit varying exposure levels. If the lighting is dimmer, operators may subjectively interpret the foliage as denser, while variations in exposure can affect the size of the grey zones. Under lower light conditions, the distinction between leaves and sky become more pronounced.

In addition, CAN-EYE's edge processing demonstrates a lack of precision, frequently introducing erroneous pixel clusters along sky boundaries (Supplementary Figure 8), likely due to a programming artifact. These flaws directly contribute to systematic biases in true PAI, resulting in a consistent overestimation of LAI. Previous studies have documented similar classification errors in LAI measurements (Duveiller and Defourny, 2010; Zhu et al., 2023).

Secondly, CAN-EYE relies on manually set thresholds (such as the gamma factor), to optimize classification results. However, this process lacks a standardization. Studies have demonstrated that threshold variations can cause gap fraction deviations of up to 17% (Xie et al., 2023). This methodological inconsistency limits the tool's applicability for multi-site and long-term monitoring studies.

By contrast, ilastik utilizes a random forest model which could be automatically applied to all photos, thereby significantly mitigating the subjectivity issues associated with manual classification. Another key strength is its ability to categorize image pixels into three classes: sky, leaves, and twigs. Unlike traditional binary classification methods, where leafless canopy (but full of twigs) is often misclassified as leaves leading to LAI overestimation, particularly in savanna ecosystems (Supplementary Figure 9). Ilastik's ternary annotation can identifies twigs beyond leaves and sky. This approach effectively eliminates the misclassification of leafless canopy as leaves, thereby substantially improving LAI

measurement accuracy in woody savanna or dry forests in the dry season, when part of the tree community shed all leaves. Note that this is different to previous studies on identifying stems and branches of conifer using multispectral images (Kucharik et al., 1998). Ilastik still recognizes main stems as leaves.

### *Efficiency and accuracy*

Ilastik demonstrates significant efficiency advantages. With CAN-EYE, processing images for a given plot-month typically requires between 2 to 20 minutes, depending on image complexity, operator experience, and computer performance. By contrast, ilastik requires training on only approximately 20 representative images to generate a high-quality model, enabling fully automated, unmanned processing thereafter. This efficiency has been further validated in other ecological data processing applications (Horning et al., 2020), highlighting its potential for broader scientific use. Moreover, the seasonal variation of LAI derived from ilastik closely tracks rainfall patterns, and its spatial distributions align consistently with expected aboveground biomass differences across sites.

### *A low cost, coding free, and wide applicable protocols for research equity*

As demonstrated above, using an AI tool for leaves-sky segmentation can considerably reduce subjective errors and improve consistency, both of which are critically important for delineating subtle spatial and temporal variations in tropical forests LAI. In fact, many previous studies have proposed new AI methods for LAI calculation, demonstrating higher accuracy and efficiency than traditional methods (Yamaguchi et al., 2020). However, tropical forests researchers (particularly those in developing countries where most tropical forests are located) often lack high-performance computing resources and coding expertise, which limits the application of complex AI methods (Ha, 2024; Sarkar and Chapman, 2021). To facilitate

comparison across time and study sites, there is an urgent need for a widely applicable AI-based LAI protocol.

Against this backdrop, our protocol offers a low-cost, flexible, and user-friendly solution for applying AI to LAI calculation, opening new avenues for research teams with limited resources (Kreshuk and Zhang, 2019). Since both software programs in the protocol are free, the only required purchase is a digital camera with a fisheye lens, resulting in a total cost of less than £1,000 (Zhu et al., 2023). Using a smartphone with a fisheye lens is also possible, provided that the appropriate parameters are used in CAN-EYE. Moreover, ilastik uses established, classic AI algorithms that can be run on a standard commercial laptop (around £600), neither a high-performance cluster nor an advanced GPU in required (C. Sommer et al., 2011).

As we have shown, ilastik's random forest models can be applied to various forest types, including woody savanna, as the software allows personalized training based on the characteristics of different ecosystems (Obels, 2021). Thus, the protocol can be widely applied to enable site-to-site comparison while being free of subjective bias. Moreover, the protocol does not regulate the DHP images-shooting process, meaning it could be applied to photos that were already taken in the past.

The protocol’s low cost and high versatility have profound implications for global ecological research equity. Research teams in developing countries can leverage this approach to achieve precise LAI measurements with limited equipment budgets, thereby promoting greater democratization of regional ecological studies. This automated, reproducible workflow is equally suitable for research projects across various scales while also laying the solid foundation for international ecological research collaboration.

It should be noted that this comparative analysis focuses on CAN-EYE, a widely used LAI calculation software, and does not consider other LAI software such as Hemisfer. Nonetheless, ilastik could be combined with Hemisfer and other LAI calculation software. We chose CAN-EYE rather than Hemisfer because the latter is not free of charge. Hemisfer itself can process images automatically completely without supervision (called ‘batch processing’) by ‘Automatic thresholding’ (Nobis and Hunziker, 2005). However, we could not get clear seasonal pattern of LAI out of this function likely due to issues in the black-white threshold. Replacing the ‘Automatic thresholding’ function with ilastik may improve

the outcomes from Hemisfer, but testing and showing results of Hemisfer are outside the scope of this study, which nonetheless is suggested for future researchers.

## *Conclusion*

Many traditional DHP software programs rely on manual pixel classification (distinguishing between leaves and sky), which may introduce subjective errors (Y. Tong et al., 2022), while AI-based automatic methods often require coding expertise. In this study, we introduce a protocol that combines two user-friendly softwares, ilastik and CAN-EYE, to achieve AI-based automated classification and LAI calculation. By comparing this approach with traditional processing procedures, this study demonstrates the importance of using an AI-based software for the leaf-sky pixel classification step.

The protocol offers several key advantages:

(1) High accuracy: By applying the same ilastik model consistently across various study sites and measurement periods, the method reliably captures subtle changes in LAI. This approach can distinguish both interannual and seasonal variations in tropical LAI and can differentiate between tropical forest subtypes.
(2) Efficiency and consistency: Compared to traditional manual methods, this approach significantly reduces both manual processing time and subjective errors. Because the LAI outputs are not operator-dependent, they achieve high reproducibility.
(3) Accessibility and cost-effectiveness: The software package feature intuitive interfaces that require no coding skills, making them accessible to users without programming expertise. Since both software options are free, the camera and tripod represent the only required costs. Consequently, the protocol offers technical support for LAI measurement in lower-income countries, potentially enhancing ecosystem monitoring equity.

# Codes and data availability

All data and codes generated in this study have been deposited in the 'zenodo' database under accession code **[XXXX will be uploaded upon acceptance]**. The above includes the protocol. As Zenodo allows authors to archive a new version after publication. We are likely to update the protocol by uploading a new version on Zenodo. Please check the Zenodo archive for possible new versions.

# References


Baker, M., 2016. 1,500 scientists lift the lid on reproducibility. Nature 533, 452–454. https://doi.org/10.1038/533452a

Berg, S., Kutra, D., Kroeger, T., Straehle, C.N., Kausler, B.X., Haubold, C., Schiegg, M., Ales, J., Beier, T., Rudy, M., Eren, K., Cervantes, J.I., Xu, B., Beuttenmueller, F., Wolny, A., Zhang, C., Koethe, U., Hamprecht, F.A., Kreshuk, A., 2019. ilastik: Interactive machine learning for (bio)image analysis. Nat. Methods 16, 1226–1232. https://doi.org/10.1038/s41592-019-0582-9

C. Sommer, C. Straehle, U. Köthe, F. A. Hamprecht, 2011. Ilastik: Interactive learning and segmentation toolkit, in: 2011 IEEE International Symposium on Biomedical Imaging: From Nano to Macro. Presented at the 2011 IEEE International Symposium on Biomedical Imaging: From Nano to Macro, pp. 230–233. https://doi.org/10.1109/ISBI.2011.5872394

Carrasco-Benavides, M., Mora, M., Maldonado, G., Olguín-Cáceres, J., Bennewitz, E. von, Ortega-Farías, S., Gajardo, J., Fuentes, S., 2016. Assessment of an automated digital method to estimate leaf area index (LAI) in cherry trees. N. Z. J. Crop Hortic. Sci.

Chen, Q., Zheng, B., Chenu, K., Hu, P., Chapman, S.C., 2022. Unsupervised plot-scale LAI phenotyping via UAV-based imaging, modelling, and machine learning. Plant Phenomics 2022. https://doi.org/10.34133/2022/9768253

de Wasseige, C., Bastin, D., Defourny, P., 2003. Seasonal variation of tropical forest LAI based on field measurements in central african republic. Agric. For. Meteorol. 119, 181–194. https://doi.org/10.1016/S0168-1923(03)00138-2

Duveiller, G., Defourny, P., 2010. Batch processing of hemispherical photography using object-based image analysis to derive canopy biophysical variables. Int. Arch. Photogramm. Remote Sens. Spat. Inf. Sci. 38.

Fang, H., Li, W., Wei, S., Jiang, C., 2014. Seasonal variation of leaf area index (LAI) over paddy rice fields in NE China: Intercomparison of destructive sampling, LAI-2200, digital hemispherical photography (DHP), and AccuPAR methods. Agric. For. Meteorol. 198–199, 126–141. https://doi.org/10.1016/j.agrformet.2014.08.005

Fuentes, S., Palmer, A.R., Taylor, D., Zeppel, M., Whitley, R., Eamus, D., 2008. An automated procedure for estimating the leaf area index (LAI) of woodland ecosystems using digital imagery, MATLAB programming and its application to an examination

of the relationship between remotely sensed and field measurements of LAI. Funct. Plant Biol. 35, 1070. https://doi.org/10.1071/FP08045

Funk, C., Peterson, P., Landsfeld, M., Pedreros, D., Verdin, J., Shukla, S., Husak, G., Rowland, J., Harrison, L., Hoell, A., Michaelsen, J., 2015. The climate hazards infrared precipitation with stations—a new environmental record for monitoring extremes. Sci. Data 2, 150066. https://doi.org/10.1038/sdata.2015.66

Gara, T.W., Rahimzadeh-Bajgiran, P., Darvishzadeh, R., 2021. Forest leaf mass per area (LMA) through the eye of optical remote sensing: A review and future outlook. Remote Sens. 13, 3352. https://doi.org/10.3390/rs13173352

Gilardelli, C., Orlando, F., Movedi, E., Confalonieri, R., 2018. Quantifying the accuracy of digital hemispherical photography for leaf area index estimates on broad-leaved tree species. Sensors 18, 1028. https://doi.org/10.3390/s18041028

Ha, D.H., 2024. The application of artificial intelligence in addressing climate change in tropical regions, in: 2024 International Conference on Platform Technology and Service (PlatCon). Presented at the 2024 International Conference on Platform Technology and Service (PlatCon), pp. 89–94. https://doi.org/10.1109/PlatCon63925.2024.10830746

Hazarika, M.K., Yasuoka, Y., Ito, A., Dye, D., 2005. Estimation of net primary productivity by integrating remote sensing data with an ecosystem model. Remote Sens. Environ. 94, 298–310. https://doi.org/10.1016/j.rse.2004.10.004

Horning, N., Fleishman, E., Ersts, P.J., Fogarty, F.A., Wohlfeil Zillig, M., 2020. Mapping of land cover with open-source software and ultra-high-resolution imagery acquired with unmanned aerial vehicles. Remote Sens. Ecol. Conserv. 6, 487–497. https://doi.org/10.1002/rse2.144

Houborg, R., McCabe, M.F., Gao, F., 2016. A spatio-temporal enhancement method for medium resolution LAI (STEM-LAI). Int. J. Appl. Earth Obs. Geoinformation 47, 15–29. https://doi.org/10.1016/j.jag.2015.11.013

Hoyt, C.T., Gyori, B.M., 2024. The O3 guidelines: Open data, open code, and open infrastructure for sustainable curated scientific resources. Sci. Data 11, 547. https://doi.org/10.1038/s41597-024-03406-w

Imteaz, M.A., Hossain, I., 2023. Climate change impacts on ‘seasonality index’ and its potential implications on rainwater savings. Water Resour. Manag. 37, 2593–2606. https://doi.org/10.1007/s11269-022-03320-z

Jiang, C., Ryu, Y., Fang, H., Myneni, R., Claverie, M., Zhu, Z., 2017. Inconsistencies of interannual variability and trends in long□term satellite leaf area index products. Glob. Change Biol. 23, 4133–4146. https://doi.org/10.1111/gcb.13787

Jonckheere, I., Fleck, S., Nackaerts, K., Muys, B., Coppin, P., Weiss, M., Baret, F., 2004. Review of methods for in situ leaf area index determination. Agric. For. Meteorol. 121, 19–35. https://doi.org/10.1016/j.agrformet.2003.08.027

Kedron, P., Frazier, A.E., 2022. How to improve the reproducibility, replicability, and extensibility of remote sensing research. Remote Sens. 14, 5471. https://doi.org/10.3390/rs14215471

Kreshuk, A., Zhang, C., 2019. Machine learning: Advanced image segmentation using ilastik, in: Rebollo, E., Bosch, M. (Eds.), Computer Optimized Microscopy: Methods and Protocols. Springer, New York, NY, pp. 449–463. https://doi.org/10.1007/978-1-4939-9686-5_21

Kucharik, C.J., Norman, J.M., Gower, S.T., 1998. Measurements of branch area and adjusting leaf area index indirect measurements. Agric. For. Meteorol. 91, 69–88. https://doi.org/10.1016/S0168-1923(98)00064-1

Li, H., Zhou, Y., Zhao, X., Zhang, X., Liang, S., 2024. A dataset of 0.05-degree leaf area index in China during 1983–2100 based on deep learning network. Sci. Data 11, 1122. https://doi.org/10.1038/s41597-024-03948-z

Li, X., Du, H., Mao, F., Zhou, G., Han, N., Xu, X., Liu, Y., Zhu, D., Zheng, J., Dong, L., Zhang, M., 2019. Assimilating spatiotemporal MODIS LAI data with a particle filter algorithm for improving carbon cycle simulations for bamboo forest ecosystems. Sci. Total Environ. 694, 133803. https://doi.org/10.1016/j.scitotenv.2019.133803

Luiselli, L., Fa, J.E., 2019. Ecology and conservation of west african forests: An introduction. Acta Oecologica, Guinean Forests of West and Central Africa: Ecology and Conservation 94, 1–2. https://doi.org/10.1016/j.actao.2018.04.004

Ma, Y., Wang, W., Jin, S., Li, Haoxin, Liu, B., Gong, W., Fan, R., Li, Hui, 2023. Spatiotemporal variation of LAI in different vegetation types and its response to climate change in China from 2001 to 2020. Ecol. Indic. 156, 111101. https://doi.org/10.1016/j.ecolind.2023.111101

Malhado, A.C.M., Costa, M.H., de Lima, F.Z., Portilho, K.C., Figueiredo, D.N., 2009. Seasonal leaf dynamics in an amazonian tropical forest. For. Ecol. Manag. 258, 1161–1165. https://doi.org/10.1016/j.foreco.2009.06.002

Malhi, Y., Girardin, C., Metcalfe, D.B., Doughty, C.E., Aragão, L.E.O.C., Rifai, S.W., Oliveras, I., Shenkin, A., Aguirre-Gutiérrez, J., Dahlsjö, C.A.L., Riutta, T., Berenguer, E., Moore, S., Huasco, W.H., Salinas, N., Da Costa, A.C.L., Bentley, L.P., Adu-Bredu, S., Marthews, T.R., Meir, P., Phillips, O.L., 2021. The global ecosystems monitoring network: Monitoring ecosystem productivity and carbon cycling across the tropics. Biol. Conserv. 253, 108889. https://doi.org/10.1016/j.biocon.2020.108889

Nair, A., Ajith Joseph, K., Nair, K.S., 2014. Spatio-temporal analysis of rainfall trends over a maritime state (kerala) of India during the last 100 years. Atmos. Environ. 88, 123–132. https://doi.org/10.1016/j.atmosenv.2014.01.061

Nobis, M., Hunziker, U., 2005. Automatic thresholding for hemispherical canopy-photographs based on edge detection. Agric. For. Meteorol. 128, 243–250. https://doi.org/10.1016/j.agrformet.2004.10.002

Obels, P., 2021. Monitoring plant growth in vertical farms using computer vision. Eindhoven University of Technology.

Prance, G.T., 1984. The vegetation of africa. by F. White. Brittonia 36, 273–273. https://doi.org/10.2307/2806524

Pyare, P.P., Henning, B., 2012. An efficient approach to standardizing the processing of hemispherical images for the estimation of forest structural attributes. Agric. For. Meteorol. 160, 1–13. https://doi.org/10.1016/j.agrformet.2012.02.007

Sarkar, D., Chapman, C.A., 2021. The smart forest conundrum: Contextualizing pitfalls of sensors and AI in conservation science for tropical forests. Trop. Conserv. Sci. 14, 19400829211014740. https://doi.org/10.1177/19400829211014740

Sumida, A., Watanabe, T., Miyaura, T., 2018. Interannual variability of leaf area index of an evergreen conifer stand was affected by carry-over effects from recent climate conditions. Sci. Rep. 8, 13590. https://doi.org/10.1038/s41598-018-31672-3

Veryard, R., Wu, J., O'Brien, M.J., Anthony, R., Both, S., Burslem, D.F.R.P., Chen, B., Fernandez-Miranda Cagigal, E., Godfray, H.C.J., Godoong, E., Liang, S., Saner, P., Schmid, B., Sau Wai, Y., Xie, J., Reynolds, G., Hector, A., 2023. Positive effects of tree diversity on tropical forest restoration in a field-scale experiment. Sci. Adv. 9, eadf0938. https://doi.org/10.1126/sciadv.adf0938

Wang, Y.-P., Zhang, L., Liang, X., Yuan, W., 2024. Coupled models of water and carbon cycles from leaf to global: A retrospective and a prospective. Agric. For. Meteorol. 358, 110229. https://doi.org/10.1016/j.agrformet.2024.110229

Wu, J., Albert, L.P., Lopes, A.P., Restrepo-Coupe, N., Hayek, M., Wiedemann, K.T., Guan, K., Stark, S.C., Christoffersen, B., Prohaska, N., Tavares, J.V., Marostica, S., Kobayashi, H., Ferreira, M.L., Campos, K.S., Da Silva, R., Brando, P.M., Dye, D.G., Huxman, T.E., Huete, A.R., Nelson, B.W., Saleska, S.R., 2016. Leaf development and demography explain photosynthetic seasonality in Amazon evergreen forests. Science 351, 972–976. https://doi.org/10.1126/science.aad5068

Wu, J., Serbin, S.P., Xu, X., Albert, L.P., Chen, M., Meng, R., Saleska, S.R., Rogers, A., 2017. The phenology of leaf quality and its within-canopy variation is essential for accurate modeling of photosynthesis in tropical evergreen forests. Glob. Change Biol. 23, 4814–4827. https://doi.org/10.1111/gcb.13725

Wu, X., Niu, C., Liu, X., Hu, T., Feng, Y., Zhao, Y., Liu, S., Liu, Z., Dai, G., Zhang, Y., Van Meerbeek, K., Wu, J., Liu, L., Guo, Q., Su, Y., 2024. Canopy structure regulates autumn phenology by mediating the microclimate in temperate forests. Nat. Clim. Change 1–7. https://doi.org/10.1038/s41558-024-02164-2

Xie, X., Yang, Y., Li, W., Liao, N., Pan, W., Su, H., 2023. Estimation of leaf area index in a typical northern tropical secondary monsoon rainforest by different indirect methods. Remote Sens. 15, 1621. https://doi.org/10.3390/rs15061621

Y. Tong, Z. Jiao, X. Zhang, S. Yin, J. Guo, 2022. An improved method for estimating clumping index by digital hemispheric photography with field measurements. IEEE Geosci. Remote Sens. Lett. 19, 1–5. https://doi.org/10.1109/LGRS.2022.3216274

Yamaguchi, T., Tanaka, Y., Imachi, Y., Yamashita, M., Katsura, K., 2020. Feasibility of combining deep learning and RGB images obtained by unmanned aerial vehicle for leaf area index estimation in rice. Remote Sens. 13, 84. https://doi.org/10.3390/rs13010084

Yan, G., Hu, R., Luo, J., Weiss, M., Jiang, H., Mu, X., Xie, D., Zhang, W., 2019. Review of indirect optical measurements of leaf area index: Recent advances, challenges, and perspectives. Agric. For. Meteorol. 265, 390–411. https://doi.org/10.1016/j.agrformet.2018.11.033

Yan, K., Wang, J., Peng, R., Yang, K., Chen, X., Yin, G., Dong, J., Weiss, M., Pu, J., Myneni, R.B., 2024. HiQ-LAI: A high-quality reprocessed MODIS leaf area index dataset with

better spatiotemporal consistency from 2000 to 2022. Earth Syst. Sci. Data 16, 1601–1622. https://doi.org/10.5194/essd-16-1601-2024

Yan, K., Zou, D., Yan, G., Fang, H., Weiss, M., Rautiainen, M., Knyazikhin, Y., Myneni, R.B., 2021. A bibliometric visualization review of the MODIS LAI/FPAR products from 1995 to 2020. J. Remote Sens. 2021. https://doi.org/10.34133/2021/7410921

Yang, S., Peng, N., Zhai, D., Tao, Y., He, Q., Mu, X., Li, Y., Fan, W., 2023. Fisheye-Based Forest LAI Field Measurements for Remote Sensing Validation at High Spatial Resolution. IEEE Geosci. Remote Sens. Lett. 20, 1–5. https://doi.org/10.1109/LGRS.2023.3308369

Zhang-Zheng, H., Adu-Bredu, S., Duah-Gyamfi, A., Moore, S., Addo-Danso, S.D., Amissah, L., Valentini, R., Djagbletey, G., Anim-Adjei, K., Quansah, J., Sarpong, B., Owusu-Afriyie, K., Gvozdevaite, A., Tang, M., Ruiz-Jaen, M.C., Ibrahim, F., Girardin, C.A.J., Rifai, S., Dahlsjö, C.A.L., Riutta, T., Deng, X., Sun, Y., Prentice, I.C., Oliveras Menor, I., Malhi, Y., 2024a. Contrasting carbon cycle along tropical forest aridity gradients in west africa and amazonia. Nat. Commun. 15, 3158. https://doi.org/10.1038/s41467-024-47202-x

Zhang-Zheng, H., Deng, X., Aguirre-Gutiérrez, J., Stocker, B.D., Thomson, E., Ding, R., Adu-Bredu, S., Duah-Gyamfi, A., Gvozdevaite, A., Moore, S., Oliveras Menor, I., Prentice, I.C., Malhi, Y., 2024b. Why models underestimate west african tropical forest primary productivity. Nat. Commun. 15, 9574. https://doi.org/10.1038/s41467-024-53949-0

Zhu, L., Guan, P., Liu, W., Zheng, Y., 2023. Optimization of lai estimation method based on smartphones with fisheye lens. Int. J. Circuits Syst. Signal Process. 17, 112–122. https://doi.org/10.46300/9106.2023.17.14

Zou, L., Stan, K., Cao, S., Zhu, Z., 2023. Dynamic global vegetation models may not capture the dynamics of the leaf area index in the tropical rainforests: A data-model intercomparison. Agric. For. Meteorol. 339, 109562. https://doi.org/10.1016/j.agrformet.2023.109562

# Acknowledgement

We thank Vivian Fe Ursula Schader, Ina Pelster, and Katrin Wilhelm for their trail of the protocol and insightful comments. M.T. and L.F. was supported by Second-class Scholarship (by China Agricultural University, Beijing). H.Z-Z was supported as part of the Next Generation Ecosystem Experiments-Tropics, funded by the U.S. Department of Energy, Office of Science, Office of Biological and Environmental Research. This work is a product of the Global Ecosystems Monitoring (GEM) network (gem.tropicalforests.ox.ac.uk). Fieldwork was funded by grants from the UK Natural Environment Research Council

(NE/I014705/1 and NE/P001092/1) to Y.M. and Africa Oxford Initiative Catalyst Grant to H.Z. We also acknowledge the Wildlife Division of the Forestry Commission in Ghana as well as the many field assistants who helped with data collection from the field.

# Author contributions

M.T., H.Z., conceived the study. S.A.B., A.D.G., H.Z., Y.M. collected field data. M.T., L.F.N., T.M.X, H.Z., did the modelling work. M.T., T.M.X, H.Z., carried out data analysis. H.Z., C.D.,Y.M., revised the manuscript. M.T. wrote the paper with inputs and revisions from all co-authors.

### *Competing interest statement*

The authors declare no competing interests.

### *Inclusion & Ethics statement*

Local researchers were involved throughout the research process, with clear roles and responsibilities agreed upon, particularly with contributions from the Forestry Research Institute of Ghana. The research was locally relevant and determined in collaboration with local partners. Capacity-building workshops were organized during the research process. Local and regional research relevant to the study is cited, as evidenced by the references to West Africa specific studies. Risk management plans were made for the fieldwork following the universities' regulations.